S. Cerri, M.A. Bohn, K. Menke, L. Galfetti
Characterization of ADN/GAP-Based and ADN/Desmophen-Based Propellant Formulations and Comparison with AP Analogues
Propellants, Explosives, Pyrotechnics, Vol. 39, N. 2, 2014, p. 192-204
doi:10.1002/prep.201300065

Characterization of ADN/GAP-Based and ADN/ Desmophen®-Based Propellant Formulations and Comparison with AP Analogues

Sara Cerri[1], Manfred A. Bohn[2], Klaus Menke[2], Luciano Galfetti[3]

1 Independent Consultant, 28060, Cureggio, Italy
2 Fraunhofer Institut fuer Chemische Technologie (ICT), 76318, Pfinztal-Berghausen, Germany
3 Dipartimento di Scienze e Tecnologie Aerospaziali, Politecnico di Milano, 20156, Milano, Italy

Abstract

Several ADN-based rocket propellant formulations containing different pre-polymers (GAP diol/triol, Desmophen® 2200), curing agents (BPS, Desmodur® N100, Desmodur® N3400), plasticizers (BDNPA-F, TMETN), and filler types (Al, HMX) have been manufactured. Propellant formulations were characterized by tensile tests, SEM analyses and DMA measurements. The study has focused on characterizations of the propellants in terms of evaluation of the strength and strain capability, investigation of the presence/absence of dewetting phenomena, compatibility issues and evaluation of the glass transition temperature. Ammonium perchlorate-based propellant formulations have also been manufactured and analyzed in order to make comparisons. Aging was investigated using mass loss measurements.

1 Introduction

Rocket propellant formulations based on ammonium perchlorate (AP), aluminum (Al) and hydroxyl terminated polybutadiene (HTPB) or similar pre-polymers are mainly used in the current western rocket motor boosters. These formulations show good mechanical and ballistic properties, but the combustion of AP poses severe corrosion and environmental risks due to the release of hydrogen chloride in the atmosphere. The increasing interest of the scientific community in the environmental issues and in the disposal of energetic materials [1] has focused the research on the development of smokeless, low-signature, environmentally friendly or reduced polluting solid rocket propellant formulations having ballistic, mechanical and aging properties similar to the current used AP/Al-based propellants.
Several ADN-based and AP-based propellant formulations containing different filler types (aluminum powders, HMX particles) were investigated in order to evaluate the compatibility of ADN with the considered pre-polymers (GAP diol/triol, Desmophen® D2200), plasticizers (BDNPA-F, TMETN) and curing agents (bispropargylsuccinate, Desmodur® N100, Desmodur® N3400), the effectiveness of the bonding agent (HX-880) and the mechanical properties. An aging investigation has also been conducted using mass loss measurements. This paper is the second one in a series of papers. For the first one see Ref. 2.

2 Experimental Section

2.1 Formulations

All propellant formulations have been manufactured at Fraunhofer ICT. Details of the formulations are shown in Table 1, Table 2, and Table 3. For convenience, the GAP-based propellants are called GAPxx, whereas the Desmophen®-based ones are named D2200xx. Depending on the considered oxidizer, the prefix ADN or AP is added. The ADN prills were manufactured at Fraunhofer ICT with a mean particle size of 106 µm. Uncoated and unstabilized prills were used.

Table 1. Composition of the ADN-GAPxx formulations.

Components		**ADN-V127**	**ADN-V128**	**ADN-V130**
ADN prills 106 µm	[m.-%]	56.00	56.00	59.20
HMX 5 µm	[m.-%]	–	–	10.00
µAl 8 µm	[m.-%]	10.00	5.00	–
nAl 100–200 nm	[m.-%]		5.00	–
GAP-diol	[m.-%]	18.58	18.58	14.51
GAP-triol	[m.-%]	3.625	3.625	2.830
BDNPA-F	[m.-%]	8.10	8.10	10.22
Stabilizers	[m.-%]	1.60	1.60	1.60
BPS	[m.-%]	2.095	2.095	1.640
Solid load	[m.-%]	66.00	66.00	69.20
Plasticizer of binder	[m.-%]	25.00	25.00	35.00
R_{eq} (C≡C/“OH”)	[-]	1.00	1.00	1.00
ρ_{th}	[g cm^{-3}]	1.653	1.653	1.636
O. B.	[%]	−30.01	−30.01	−17.17

Table 2. Composition of the AP-GAPxx formulations.

Components		**AP-13**	**AP-14**	**AP-15**
AP 45 µm	[m.-%]	18.66	18.66	18.66
AP 200 µm	[m.-%]	37.34	37.34	37.34
HMX 5 µm	[m.-%]	10.00	10.00	10.00
GAP-diol	[m.-%]	16.37	18.68	16.26
GAP-triol	[m.-%]	3.20	–	3.17
BDNPA-F	[m.-%]	10.80	10.80	10.80
HX-880	[m.-%]	–	–	0.14
Stabilizers	[m.-%]	1.60	1.60	1.60
BPS	[m.-%]	2.03	–	2.03
Desmodur® N100	[m.-%]	–	2.92	–
Solid load	[m.-%]	66.00	66.00	66.00
Plasticizer of binder	[m.-%]	33.33	33.33	33.33
R_{eq} (C≡C/“OH”)	[-]	1.10	1.00	1.00
ρ_{th}	[g cm^{-3}]	1.682	1.682	1.682
O. B.	[%]	−15.35	−16.81	−15.35

Table 3. Composition of the D2200xx formulations.

Components		ADN-V142	ADN-V144	AP-11	AP-12
ADN prills 106 µm	[m.-%]	56.00	56.00	–	–
AP 45 µm	[m.-%]	–	–	18.66	18.66
AP 200 µm	[m.-%]	–	–	37.34	37.34
HMX 5 µm	[m.-%]	10.00	–	–	10.00
µAl 8 µm	[m.-%]	–	10.00	10.00	–
Desmophen® D2200	[m.-%]	17.42	17.42	17.42	17.42
TMETN+0.5 % 2-NDPA	[m.-%]	10.80	10.80	10.80	10.80
HX-880	[m.-%]	0.14	0.14	0.14	0.14
Stabilizers	[m.-%]	1.60	1.60	1.60	1.60
Desmodur® N3400	[m.-%]	4.04	4.04	4.04	4.04
Solid load	[m.-%]	66.00	66.00	66.00	66.00
Plasticizer of binder	[m.-%]	33.33	33.33	33.33	33.33
R_{eq} (NCO/OH)	[-]	1.00	1.00	0.99	0.99
ρ_{th}	[g cm^{-3}]	1.589	1.628	1.689	1.646
O. B.	[%]	−30.89	−37.63	−26.27	−32.97

Formulations were prepared in a vertical kneader (Drais T FHG, Germany) having a 5 L volume and cured in an electrical oven cabinet (company Memmert, Germany). The ADN-GAPxx formulations were processed at 50 °C and cured for 2 d at 60 °C. The AP-GAPxx formulations were processed at 40 °C and cured for 2 d at 60 °C. The ADN-D2200xx formulations were processed at 50 °C and cured 1 d at 60 °C. The AP-D2200xx formulations were processed at 50 °C and cured 1 d at 60 °C.

2.1.1 GAP-Based Formulations

GAPxx formulations are divided into those containing ADN as oxidizer (Table 1) and those containing AP (Table 2). GAP diol and triol were cured with bispropargylsuccinate (BPS), a diacetylene derivative made by esterification of succinic acid with propargyl alcohol [3]. Only the formulation named AP-14 was cured with the formally trifunctional isocyanate Desmodur® N100 (HDI biuret).
BDNPA-F was used as plasticizer for the ADN-GAPxx formulations and TMETN was added to the AP-GAPxx propellants. All GAPxx formulations contained a mixture of stabilizers of type Akardit II, MNA and a zeolite, see also Ref. 4.
ADN-GAPxx formulations have been manufactured with the same equivalent ratio, however differences occur for the AP-GAPxx propellants. During the curing process the triple bonds (C≡C) of BPS react in [1,3] dipolar cycloaddition (so-named Huisgen reaction) with the azido groups of GAP to form cross-links via triazoles and this type of curing is then named triazole curing. Therefore a pseudo OH group (named “OH”) was considered in the equivalent ratio R_{eq}. To evaluate R_{eq}, the real OH groups of GAP have been the base. Stability and compatibility of BPS with ADN were investigated and found appropriate [5]. Details on the curing process can be found in Ref. 5.

2.1.2 Desmophen® D2200-Based Formulations

The compositions of the polyesterurethane formulations are shown in Table 3. All formulations contain 0.14 m.-% of bonding agent of type HX-880 (company Mach I, Inc., King of Prussia, PA, USA), see list of abbreviations.

2.2 Characterization Techniques

2.2.1 Tensile Tests

The mechanical behavior of the formulations was characterized with a ZWICK UPM 1476 tensile test machine. JANNAF dogbone samples (125 mm length, 25 mm width, 10 to 12 mm thickness) were used in uniaxial tensile tests at room temperature and atmospheric pressure at one strain rate of 0.0167 s^{-1}. During each test the applied force and the elongation of the gauge length were recorded by a load cell and an extensometer, respectively. The maximum corrected stress (σ_{corr}) and the natural or logarithmic strain, also called Hencky strain (ε_{log}), have been evaluated.

2.2.2 SEM Measurements

Scanning electron microscopy (SEM) analyses were performed using the scanning electron microscope Supra 55 VP manufactured by company ZEISS, Germany. Slices of propellants were cut after the tensile tests to visually investigate the absence or presence of dewetting phenomena.

2.2.3 Dynamic Mechanical Analysis (DMA)

Dynamic mechanical measurements were carried out in torsion mode using a DMA instrument of type ARES® (Advanced Rheometric Expansion System) manufactured by Rheometric Scientific (now belonging to Waters, Inc., BU TA Instruments). A liquid nitrogen cooling accessory was used for the low and high temperature operations.
Samples were rectangular bars of 10 mm wide, 4 to 5 mm thick, and 30 mm long. The temperature range was −80 °C to +80 °C, with step-wise heating by 1 K min^{-1} and a soak time of 28 s. Specimens were tested at four deformation frequency values: 0.1, 1.0, 10.0, 30.0 Hz. These propellants are softer than the HTPB/AP/Al-based ones investigated in a previous study [2] due to the used binders and the low solid load. A strain control equal to 0.0012 was too low for having good experimental results, especially at temperature values above room temperature. Therefore, two strain controls have been used: 0.00237 from −80 °C up to +15 °C, and 0.01 from +16 °C to +80 °C. Measurement reproducibility is very high, so only one sample was used. In case of anomalous behavior a second measurement was performed.

2.2.4 Mass Loss Measurements

1 g of sample was stored in glass vials with glass stoppers loosely inserted at different isothermal temperature values. Usually samples are cut in small pieces of about 2 mm cubes. For each chosen temperature two samples were considered. Stoppers were not fixed by clamping and not sealed with grease, so gas exchange could take place. The weighing was done offline with an analytical balance from Mettler Toledo in appropriate time intervals, at least twice a week.
The behavior of the propellant formulations is strongly influenced by the presence of ADN, therefore also the aging of ADN prills was analyzed at low and high temperature values by mass loss. The applied isothermal aging temperature values were:

i. 85 °C for the AP-D2200xx formulations;
ii. 65 °C, 80 °C, 85 °C for the ADN-GAPxx and ADN-D2200xx formulations;
iii. 35 °C, 40 °C, 50 °C, 60 °C, 65 °C, 70 °C, 75 °C, 80 °C, 85 °C for the ADN prills.

3 Results and Discussion

The investigated propellants have a lower solid load than the standard AP/HTPB-based formulations, typical values are about 65 m.-% and 85 m.-%, respectively. This was due to a technical limitation. ADN crystals are available in a needle shape, therefore the morphology must be improved. Prilling techniques have been developed to convert the ADN crystals to spherical particles either in suspension in an inert fluid or in a gas stream. The ADN prills used in this study were processed at Fraunhofer ICT (details of the prilling process can be found elsewhere [6]) and had an average particle size of 60–120 μm. Propellant ballistic properties are influenced to a greater degree by the oxidizer type and the particle distribution than by the metal fuel content which increases the flame temperature [7]. Recent results [8] have shown that it is possible to produce ADN particles with an adequate particle size by combining the micro reaction technique and the ADN emulsion crystallization process. Because at the time of this study multimodal ADN distributions were not available, the multipacking density approach could not be used and the only possibility to achieve higher solid load, density and performance of the propellants was obtained by adding another filler, here HMX or Al have been taken.

3.1 Formulations

The first three formulations of Table 1 have the same solid load (66 m.-%) and filler content (10 m.-%) but different filler types: ADN-V127 contains only μAl; ADN-V128 has a mixture of μAl and nAl; ADN-V129 has HMX. Therefore, the effect of the filler type can be investigated considering these propellants. The last formulation, ADN-V130, contains the same filler content but a little higher oxidizer amount (59.2 m.-%). By comparing it with ADN-V129 the effect of the solid load on the mechanical properties can be investigated. AP was used in the comparative formulations (Table 2). It was processed as received from SNPE with two average particle sizes. The solid load was maintained constant (56 m.-%) and only HMX was added. By comparing the AP-GAPxx formulations among them and with the ADN-GAPxx formulations, the effectiveness of the curing agents (AP-13/BPS vs. AP-14/Desmodur® N100) and of the polyol-amine type bonding agent (AP-13/ no b.a. vs. AP-15/HX-880), as well as the influence of the oxidizer type (AP-13/AP vs. ADN-V129/ADN) can be studied.
The first two formulations of Table 3 contain ADN as oxidizer and the same solid load (66 m.-%) and filler content (10 m.-%) but different filler type: ADN-V142 contains HMX, whereas ADN-V144 has μAl. Therefore the effect of the filler type can be investigated. The last two AP-based formulations have the same solid load but contain bimodal AP particles: AP-11 contains μAl, while AP-12 has HMX. As for the GAPxx formulations, AP formulations were used for comparison.

3.2 Mechanical Properties

Figure 1 presents the maximum of corrected stress (σ_{corr}) and strain capability (ε_{log}) map of the investigated materials (GAPxx, D2200xx) tested at 0.0167 s^{-1}. Strain capability is here defined as the strain at maximum of corrected stress. The same definition has been applied also in Refs. 2, 9. For comparison, two "state-of-the-art" formulations, represented by HTPB/AP/Al-based propellant formulations named AV03 and AV04 in Refs. 2, 9, were also included.

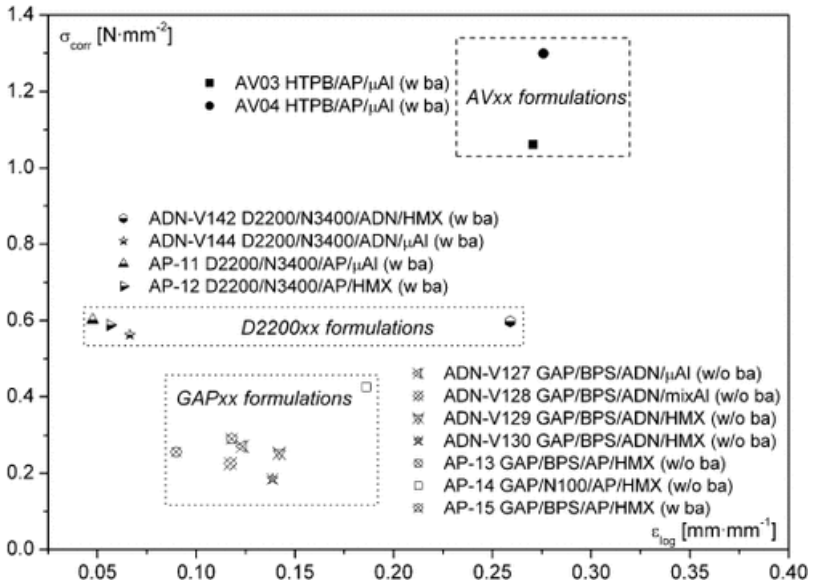

Figure 1 Maximum of corrected stress and natural strain capability map of the D2200xx and GAPxx formulations and comparison with the AVxx (state-of-the-art) formulations tested at 0.0167 s^{-1}.

The map shows four regions:

i. HTPB-based materials (AVxx): high σ_{corr} and high ε_{log};
ii. AP-D2200xx, ADN-V144 (ADN-D2200xx/μAl): intermediate σ_{corr} and low ε_{log};
iii. ADN-V142 (ADN-D2200xx/HMX): intermediate σ_{corr} and high ε_{log};
iv. GAPxx: low σ_{corr} and low ε_{log}.

The replacement of ADN by AP at the same solid load does not give remarkable changes in the maximum corrected stress but the value of the strain capability decreases (AP-13 vs. ADN-V127, ADN-V128, ADN-V129; AP-11 vs. ADN-V144; AP-12 vs. ADN-V142). The constitutive behavior of the ADN/GAP and AP/GAP-based formulations is similar as shown in Figure 2 and Figure 3.

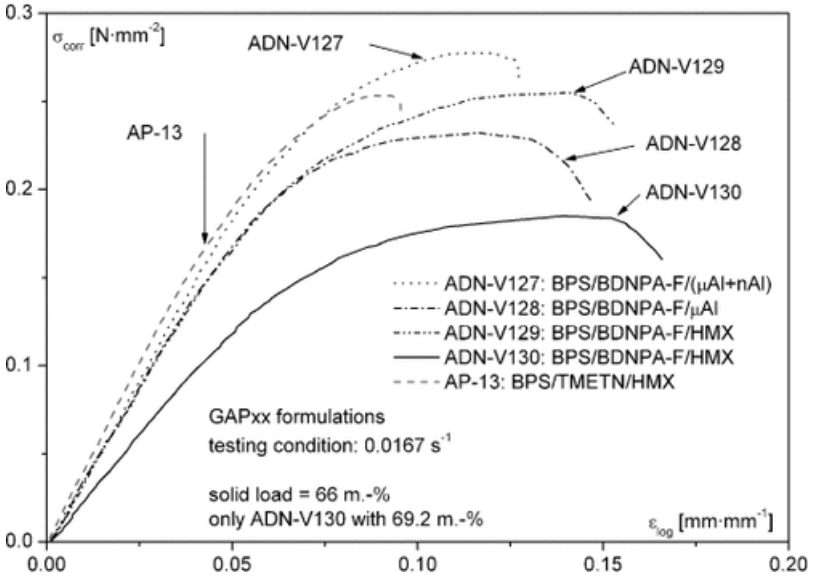

Figure 2 Tensile tests of the GAPxx formulations.

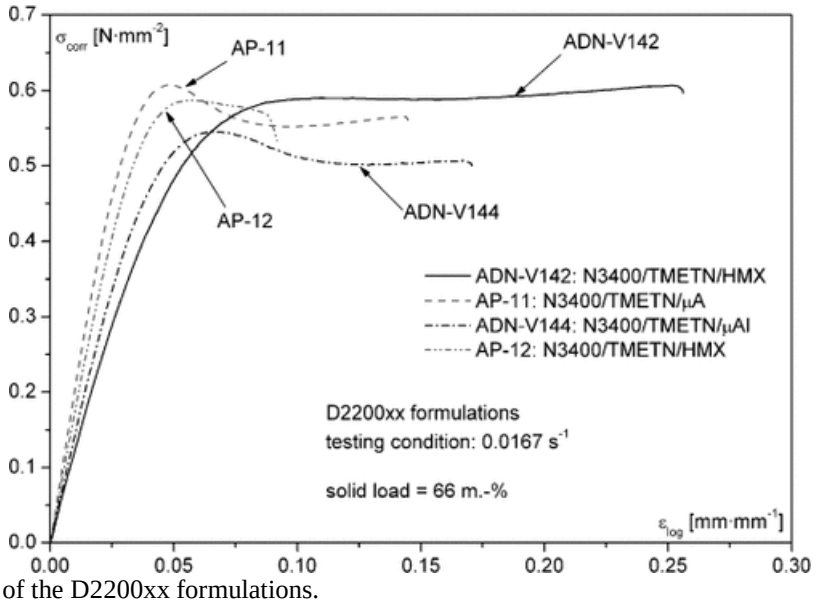

Figure 3 Tensile tests of the D2200xx formulations.

The presence of different filler types (HMX vs. Al) for the ADN-based propellant formulations does not influence the maximum corrected stress but the strain capability. Propellants containing HMX can reach higher ε_{log} ($\Delta\varepsilon_{log}$(ADN-V129)=+21 % with respect to ADN-V128; and $\Delta\varepsilon_{log}$(ADN-V142)=+290 % with respect to ADN-V144). The constitutive behavior of the ADN-GAPxx formulations is independent of the filler type, whereas the D2200xx formulations show a strong dependence (Figure 3). As already pointed out for the AVxx formulations [10], Al is an active filler: results here presented can display a possible interference of the Al particles (presence of OH-groups on the surface) on the curing process. This influence is highlighted in the ADN-D2200xx formulations.

Additional considerations can be done for the AP-GAPxx propellant formulations. The replacement of BPS (AP-13) by Desmodur® N100 (AP-14) gives a remarkable increase in the maximum corrected stress and strain capability values ($\Delta\sigma_{corr}$=+66 %, $\Delta\varepsilon_{log}$=+109 %) and a modification in the constitutive behavior 11. Thus, mechanical properties of the developmental AP/GAP/N100 (AP-14) formulation are promising even without the use of a bonding agent. The results show that a bonding agent seems not applicable for GAP/ADN-based propellants without the use of coated ADN [12–14]. However, a coating would improve the situation only if it is highly aging resistant in contact with ADN. Further on, the coating must be mechanically stable to withstand the shear forces during kneading and the thermal expansion coefficients of coating material and ADN must be matched.

The use of the bonding agent (HX-880) for the AP-15 formulation has increased the mechanical properties ($\Delta\sigma_{corr}$=+14 %, $\Delta\varepsilon_{log}$=+32 %) if compared with the AP-13 formulation. However, in spite of this gain with AP-15 over AP-13 the obtained values cannot reach the ones the HTPB/AP/Al formulations have. Incompatibility problems between HX-880 and the ADN prills have been found with the compatibility test [11, 15]. Additional work for investigating the compatibility between the oxidizer and the bonding agents will be carried on.

3.3 SEM Results

The broken surfaces, obtained after the tensile testing of the dogbone specimens, of the ADN-based formulations show the presence of fractures together with strong dewetting phenomena (Figure 4).

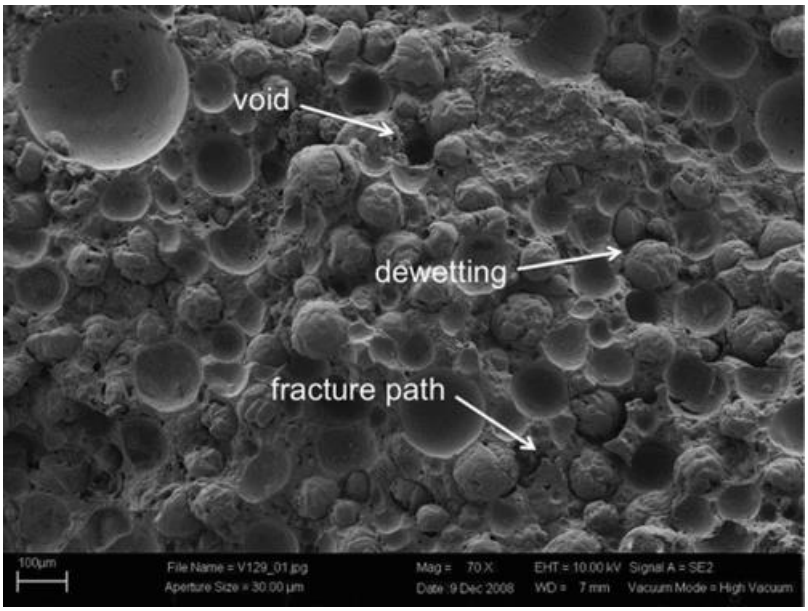

Figure 4 SEM analysis of the ADN-V129 propellant after the tensile test.

Some voids, originating from the manufacturing process and not to the detachment of the ADN particles due to the tensile load, are also clearly visible, leading to a material with a quite high porosity. This phenomenon could be caused by the high reaction heat in this curing system. The porosity and the use of BPS as curing agent are responsible for the low mechanical properties of the ADN-GAPxx formulations. Further on, if the polymeric binder does not fill the entire space not occupied by the solid filler, the flame front may proceed by connecting the voids and leading to an uncontrolled combustion process. Additional analyses published in previous publications [14, 16] have also given evidence of the presence of voids inside the prills. Further efforts are made to reduce the filler porosity by using effective stabilizers for ADN and applying suitable process technology, e.g. fluidized bed technology [17].

3.4 DMA Results

DMA measurements at 0.1 Hz of all the GAPxx and D2200xx propellant formulations show evidence of a different thermoviscoelastic behavior in comparison with the AVxx ones 2, see Figure 5. They show only one main peak in the loss factor curve tanδ, which has always a type of tailing towards the high temperature side (Figure 5, Figure 6, Figure 7).
Moreover, the investigated formulations show significantly higher glass transition temperature (T_g) values. They are 40–50 °C higher than the ones of the HTPB/AP/Al-based propellants [2, 9]. Due to the high T_g values, the ADN-based formulations may be excluded from in-service due to the climatic conditions on Earth specified in a NATO STANAG [19]. Based on the combined very cold and very hot in-service climates, which range from −54 °C to +71 °C the use of ADN propellants with presently known binders seems not possible. In case of special advantages (demands for smokeless, less polluting, less corrosive, and others) of some new formulations one may decide a selected aerial use in spite of not matching this wide temperature range.

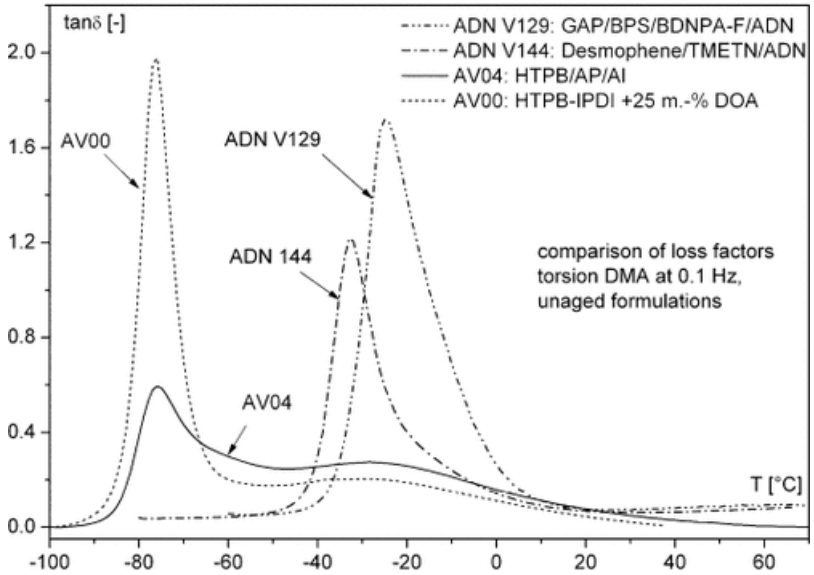

Figure 5 Comparison of loss factor data of some representatives of the investigated formulations. AV04 and AV00 have been discussed in Ref. [18].

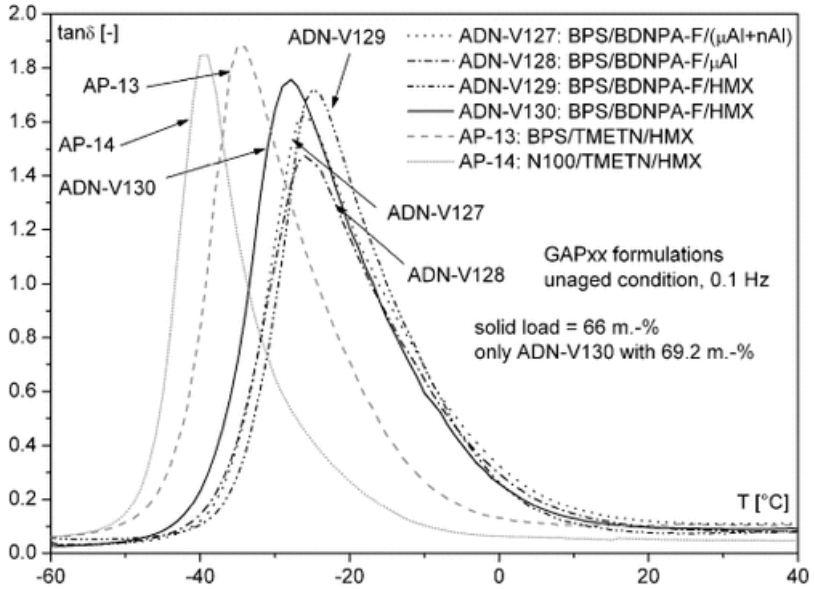

Figure 6 Loss factor of the GAPxx propellant formulations tested at 0.1 Hz.

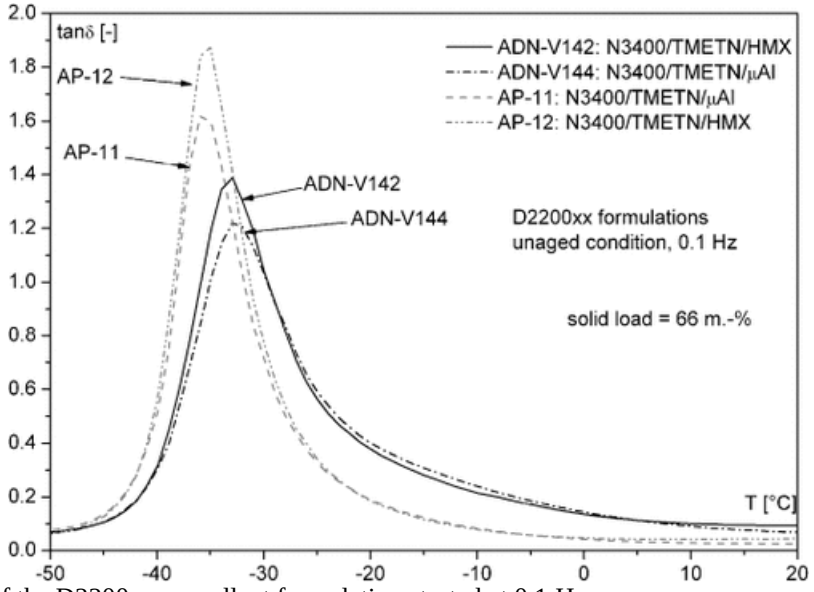

Figure 7 Loss factor of the D2200xx propellant formulations tested at 0.1 Hz.

Values of tanδ of all the formulations (both families, GAPxx and D2200xx) containing AP is higher than tanδ of the formulations containing ADN. Moreover, the loss factors of the ADN-based formulations show a dependence on the filler type. Propellants containing HMX have higher loss factor values than the ones containing aluminum: the reduction of the maximum of tanδ with Al can be explained by the presence of more intense interactions between the particles and the binders which causes a reduction in the polymer mobility. This reduction is stronger with the addition of nanoparticles (ADN-V128). Aluminum is an active filler by its OH-groups activated surface [10] and it is able to activate more intermolecular "induced dipole↔induced dipole" interactions with GAP-based and Desmophen®-based binders than HMX is able to do. In addition, hydrogen bonding between Al-OH and C-O-C elements of GAP and the ester groups of Desmophen® D2200 binder is also possible. All these interaction effects reduce the free volume, which reduces the mobility, which lowers the tanδ values and shifts the maximum of the loss factor to higher temperature values.
The polyesterurethane-based materials D2200xx show lower T_g values than the ADN-GAPxx propellants (Table 4, Table 5). Moreover, all the AP-based propellants tend to show lower glass transition temperature values than the corresponding ADN formulations. The tanδ distributions of the ADN-GAPxx formulations are quite narrow and this tendency is maintained for all the deformation frequencies applied. But the peak width at half peak height is for the AP analogues smaller than for the ADN formulations. The replacement of BPS by Desmodur® N100, the increase of the solid content (additional amount of ADN for ADN-V130) and the replacement of ADN by AP decrease the T_g value.

Table 4. T_g of the investigated GAPxx formulations.

Propellants		**$T_{g(0.1Hz)}$**	**$T_{g(1.0Hz)}$**	**$T_{g(10.0Hz)}$**	**$T_{g(30.0Hz)}$**
ADN-V127	[°C]	−26.13	−21.70	−16.06	−12.85
ADN-V128	[°C]	−26.07	−21.48	−15.86	−12.48
ADN-V129	[°C]	−24.81	−20.26	−14.61	−9.24[a]
ADN-V130	[°C]	−28.06	−23.57	−17.59	−11.90[a]
AP-13	[°C]	−34.55	−30.12	−24.72	−21.91
AP-14	[°C]	−39.51	−35.66	−30.58	−27.70

[a] Measured at 56.0 Hz instead of 30 Hz.

Table 5. T_g of the investigated D2200xx formulations.

Propellants		**$T_{g(0.1Hz)}$**	**$T_{g(1.0Hz)}$**	**$T_{g(10.0Hz)}$**	**$T_{g(30.0Hz)}$**
ADN-V142	[°C]	−33.16	−29.60	−24.98	−22.25
ADN-V144	[°C]	−32.67	−28.90	−24.23	−21.56
AP-11	[°C]	−35.56	−32.31	−27.99	−25.52
AP-12	[°C]	−35.36	−32.11	−27.84	−25.46

Explanations for these features are:

i. Higher filler content may hinder the curing reaction between GAP and BPS, and the curing does not reach the level planned, which lowers T_g;
ii. A reason of the increased T_g with the use of ADN compared to AP may be a small but not negligible solubility of ADN in the binder 4 which lowers the mobility of binder chains;
iii. Bonded particles as AP create a binder shell glass transition, which may coincide with the main peak or, more probably, appear in the high temperature side of the main peak of tanδ and let the main peak more unaffected;

iv. ADN seems to create more interactions with the binder GAP because of local dipoles in its surface part of the crystals. These local dipoles are not so effective with AP, because the crystal and the molecule of AP are much more symmetrical than with ADN.

Similar statements apply for the D2200xx propellants, as well.

3.5 Aging Behavior Revealed by Mass Loss

Some aging investigations have been conducted mainly for the ADN-based propellant formulations with mass loss measurements. Additional results for the ADN-D2200xx propellants will be published [20]. During aging, AP-D2200xx propellant specimens did not change their shape but only their color. The initial yellow and olive green colors of AP-11 and AP-12, respectively, turned initially into dark green, then into dark grey and finally into black. Instead, the ADN-formulations have shown remarkable morphological modifications due to degradation phenomena of the ADN prills and of the binder (Figure 8). By increasing the thermal load, the material degradation becomes stronger.

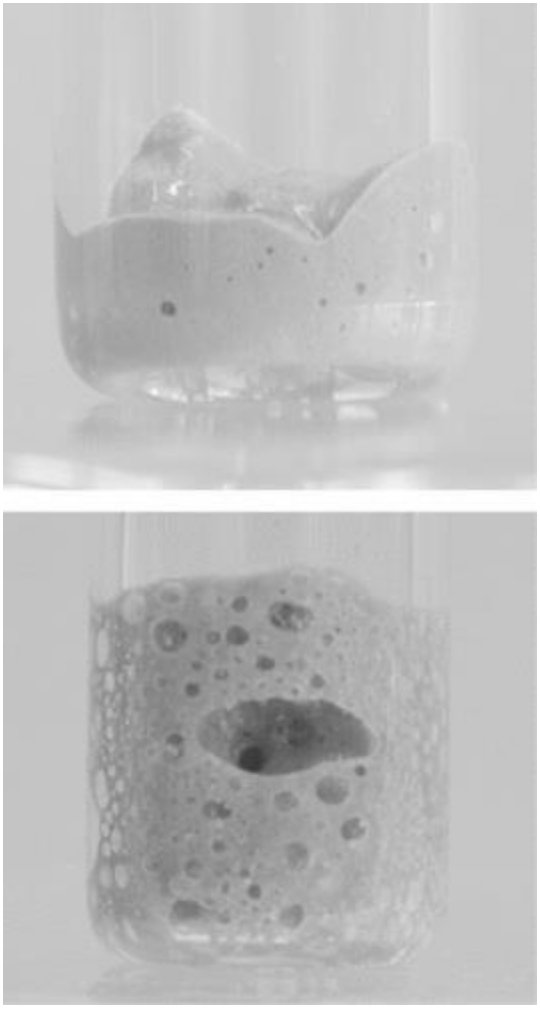

Figure 8 Specimens aged at: a) ADN-V127at 65 °C, 98 d; b) ADN-V142: 85 °C, 27 d.

The mass loss (ML) of the propellants aged at 85 °C and containing Al and HMX is shown in Figure 9. The influence of ADN has been analyzed by plotting the ML values of the ADN prills together with the propellant formulations. By comparing the behavior of the D2200xx formulations (ADN-V142 vs. AP-12, ADN-V144 vs. AP-11) the role of ADN in the decomposition process of the material is evident. Formulations containing ADN show the same accelerative behavior in ML as the prills, but their mass loss values are lower due to the less ADN content. The melting down of the GAP-BPS

based materials appears in half the time compared to the Desmophen®/N3400-based ones. The replacement of ADN by AP considerably reduces the ML value and changes also the type of the ML-trend, which means no accelerative behavior occurs.

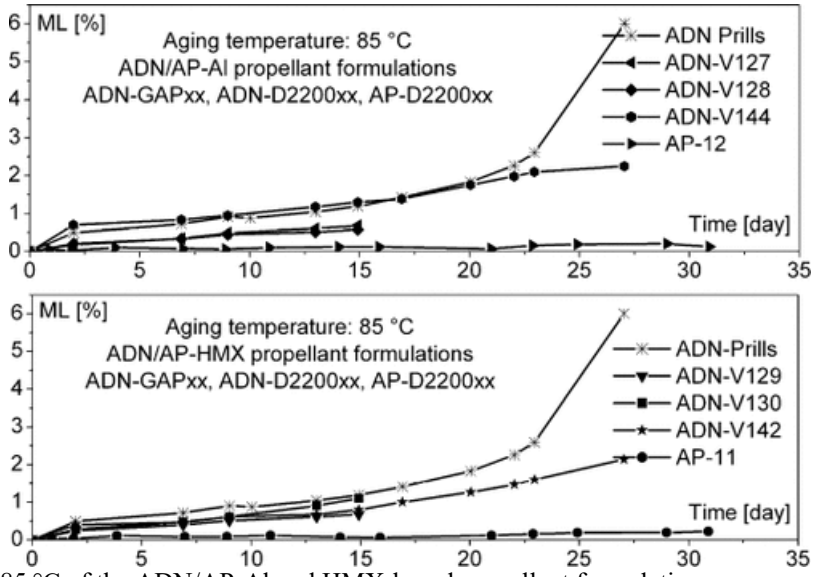

Figure 9 Mass loss at 85 °C of the ADN/AP-Al and HMX-based propellant formulations.

ML data of the used ADN prills aged at different temperature values (35–85 °C) are shown in Figure 10. Initially, all samples show an increase in ML, which is due to the volatile components such as water, but also due to unstable parts and loss in substances used as processing aid in the prilling. The ML values at 80 °C and 85 °C (later in time also at 75 °C) show, after the first quasi-instantaneous increases, a linear trend of ML with time and then an accelerated decomposition behavior, which can be described by autocatalytic modeling, see for example [21]. Below 80 °C, ADN prills do not show the autocatalytic behavior in the considered time range of 100 to 200 days used for comparison with the formulations. Beyond this time range, also the series at 75 °C show acceleration in mass loss and at 70 °C a slight indication can be found for an accelerated increase in mass loss, see Figure 10.

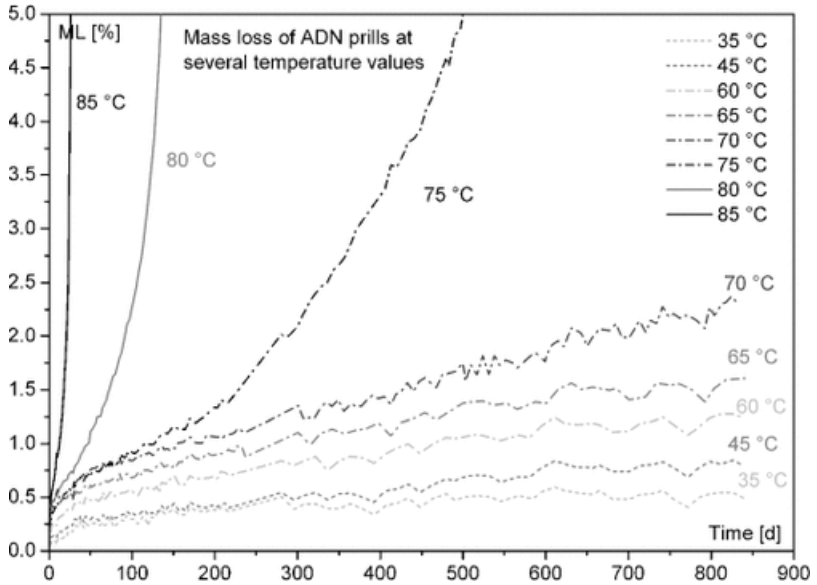

Figure 10 Extended measurement range in mass loss with the ADN prills. Also at 75 °C the acceleration in ML was found. There is indication that also at 70 °C the acceleration should start after the investigated time range.

The decomposition behavior of ADN is a complex and complicated matter. Some investigations can be found in Refs. 22–29. Manelis [22] gives a detailed discussion of the ADN decomposition and of

its peculiarities. Bohn and Grillo [25] describe the autocatalytic decomposition of ADN and analyze the possible pathway for autocatalysis by using the transition state theory. They found that protons strongly foster the decomposition process by autocatalysis. Their result is supported by the work of Kazakov et al. [27]. These authors investigated the decomposition of dissolved ADN in neutral and in acid medium and found that the activation energy for decomposition decreased from 170 kJ mol^{-1} down to 60 kJ mol^{-1}. The same low value was also found in the quantum chemical evaluation of ADN decomposition [25]. Additionally to the decomposition of ADN alone (monomolecular decay with or without autocatalysis), an 'induced' decomposition in contact with surrounding substances takes place. With GAP this is minimal and in terms of compatibility acceptable. With other substances, especially nitrate esters or proton delivering substances, the incompatibility has mostly to be stated. There is a further special feature with ADN: sometimes the incompatibility with ammonium nitrate (AN) is reported or stated. This seems not really the case. During the decomposition of ADN the AN is formed. AN lowers the melting point of ADN by formation of an eutectic, which can go down to about 60 °C. This in turn causes in part liquefaction and this in turn enhances the decomposition of ADN because the lattice energy of ADN has no longer to be overcome. Liquid ADN has a substantial lower activation energy for decomposition than solid ADN 26, about 162 kJ mol^{-1} vs. about 220 kJ mol^{-1}, and this even with stabilization in liquid phase. In the case of formation of eutectic, acceleration in mass loss is observed. This acceleration is additional and mostly somewhat before the real autocatalytic decomposition, which ADN also suffers. Rahm and Brinck 29 have considered special mechanistic pathways of decomposition. These pathways are mainly based on distortion of the dinitramide structure and also polarization of it, which happens with molecules on the ADN crystal surface. These distortions cause loss in electronic resonance of the molecule which elongates the N-N distance in dinitramide and lowers therefore its bond dissociation enthalpy and in turn the decomposition activation energy. Some ideas of stabilization and mitigation are presented also.
Due to this complexity, it is clear that such summarizing measurement quantities as mass loss and also heat generation rate cannot give a detailed and complete insight of the ADN decomposition behavior. But they can provide the overall kinetic data which are suitable to predict the use time of the propellant formulations. This is the intention used by presenting the following description of the ML data of the ADN prills. For the prills aged at 80 °C and 85 °C, three decomposition reactions were considered: the initial part of the curve was modeled with a first-order reaction (exponential course), then ML increases with time according to a pseudo-zero order reaction, which means a linear increase in ML. Finally ML shows a strong increase due to an autocatalytic decomposition reaction. For the other investigated temperature values, only the first two reactions have been taken, whereby the main part consists of only the zero order reaction. The modeling was performed with the following equations.

Model 1, "ML: Main: Zero Order+Minor: First Order"

$$ML(t,T) = OF + 100 \cdot \left\{ \frac{m_C}{m_A} \cdot (1 - a - M_k) \cdot k_0(T) \cdot t + a \cdot \left[1 - \exp(-k_V(T) \cdot t)\right] \right\} \quad (1)$$

The main part of the decomposition follows a reaction of zero order and describes the long-term behavior. The minor part is assumed to be caused by evaporation of water and other volatiles, which also may decompose. All together this is described by a reaction of first order with the rate constant **k**v.

Model 2, "ML: Main: First Order+Autocatalytic; Minor: First Order"

$$M_{Ar}(t,T) = \frac{k_1(T) + k_2(T)}{k_2(T) + k_1(T) \cdot \exp\left[(k_1(T) + k_2(T)) \cdot t\right]} \quad (2)$$

$$ML(t,T) = OF + 100 \cdot \left\{ \frac{m_C}{m_A} \cdot (1 - a - M_k) \cdot (1 - M_{Ar}(t,T)) + a \cdot \left[1 - \exp\left(-k_V(T) \cdot t\right)\right] \right\} \quad (3)$$

The main part of the decomposition follows a combined reaction of first order and autocatalytic reaction. As above, the minor part describes evaporation and/or decomposition according to a reaction of first order and occurs in the initial mass loss data.

ML(t,T)	Experimental ML as function of time and temperature;
t	Time;
T	Temperature;
m_C	Mean molar mass of escaping gases (with ADN it is mainly N_2O, m_C=44 g mol^{-1});
m_A	Mean molar mass of component A (here ADN, m_A=124 g mol^{-1});
M_k	Non-reactive impurity in ADN, M_k=0.02;
k_0	Reaction rate constant of zero order reaction in main part of model 1, [time^{-1}];
k_V	Reaction rate constant of first-order reaction in minor part of model 1 and of model 2, [time^{-1}];
a	Fraction of minor component, M_V=a·M(0);
k_1	Reaction rate constant of first-order reaction in main part of model 2, [time^{-1}];
k_2	Reaction rate constant of autocatalytic reaction in main part of model 2, [time^{-1}];
OF	Offset in ML not caused by the considered decomposition reactions (here OF=0).
ML(t_0,T)	Value of ML at time t_0=0 in evaluation with model 3; in general this quantity is dependent on temperature;
k_{ML}	Reaction rate constant in model 3, [%·time^{-1}].

A further model 3 is used and shown in Equation (4). This model is pragmatic. It considers only the linear increase directly in mass loss, which means it is zero order in mass loss. From the ML data only the linear part is used. The initial mass loss range, where the evaporation of volatiles happens, is omitted.

Model 3, "ML: Zero Order"

$$ML(t,T) = ML(t_0,T) + k_{ML}(T) \cdot t \quad (4)$$

In Table 6 the results of the evaluation with the three models is compiled. The time range of the used data and the temperature range influence the results. The temperature range has to be adapted to the course of the reaction rate constants in the Arrhenius diagrams. The data cannot be described with one set of Arrhenius parameters in the used aging temperature range. The fact that the evaluated data obtained with the models depend so much on the range of experimental data is reflecting the complex behavior of ADN. Especially the combination of topochemically fostered and real autocatalytically induced decomposition leads to such an 'incongruent' course of the mass loss. Moreover, together with reactants, as the chemical surrounding in the formulations the complexity in decomposition is enhanced further. Nevertheless, for purpose of predicting in-use times the complexity can be handled in the presented way.

Table 6. Evaluation of the mass loss data of the ADN prills using the three models. The time range of the used data and the temperature range influence the results. The average mass loss at time zero ML(0,T) has about the same value as quantity a in % of the second evaluation up tp 850 d and is also in good agreement of that of evaluation up to 200 d. The quantity a gives the fraction of the minor component, which includes processing substances used for prilling and less stable parts of ADN.

	Up to 200 d			**Up to 850 d**			**Up to 1300 d**		
T [°C]	**Model type**	**Time range of used data [d]**	**a [-]**	**Model type**	**Time range of used data [d]**	**a [-]**	**Model type**	**Time range of used data [d]**	**ML(0,T) [%]**
35	1	0–180	1.50 E-3	1	0–710	2.83 E-3	3	150–1300	3.96 E-01
45	1	0–180	2.50 E-3	1	0–710	2.67 E-3	3	200–1300	3.54 E-01
50	1	0–200	2.54 E-3	–	–	–	–	–	–
60	1	0–180	3.74 E-3	1	0–730	4.51 E-3	3	300–1100	6.40 E-01
65	1	0–200	4.66 E-3	1	0–700	5.68 E-3	3	200–1100	8.51 E-01
70	1	0–200	5.36 E-3	1	0–850	6.62 E-3	3	200–950	6.73 E-01
75	1	0–180	4.85 E-3	2	0–530	5.92 E-3	3	40–210	5.05 E-01
80	2	0–140	5.59 E-3	2	0–130	5.59 E-3	3	10–50	4.17 E-01
85	2	0–27	7.03 E-3	2	0–23	7.03 E-3	3	2–13	3.94 E-01
		Average in a	4.19 E-3		Average in a	5.16 E-3		Average in ML(0,T)	5.29 E-01

k_0 or k_1 [d^{-1}]		**k_0 or k_1 [d^{-1}]**		**k_{ML} [% d^{-1}]**	
60–85 °C		75–85 °C		70–85 °C	
E_a [kJ mol^{-1}]	57.8±1.8	E_a [kJ mol^{-1}]	120.4±28	E_a [kJ mol^{-1}]	203.0±17
Log (Z [d^{-1}])	4.761± 0.3	Log (Z [d^{-1}])	13.925±4	Log (Z [% d^{-1}])	28.189±2.5
k_0 or k_1 [d^{-1}]		**k_0 or k_1 [d^{-1}]**		**k_{ML} [% d^{-1}]**	
45–65 °C		35–70 °C		35–70 °C	
E_a [kJ mol^{-1}]	32.3±11.4	E_a [kJ mol^{-1}]	37.4±3.7	E_a [kJ mol^{-1}]	37.6±11.7
Log (Z [d^{-1}])	0.808±1.8	Log (Z [d^{-1}])	1.423±0.6	Log (Z [% d^{-1}])	2.761±1.9
k_V [d^{-1}]		**k_V [d^{-1}]**			
35–75 °C		35–75 °C			
E_a [kJ mol^{-1}]	25.5±2.9	E_a [kJ mol^{-1}]	21.7±8		
Log (Z [d^{-1}])	3.175±0.5	Log (Z [d^{-1}])	2.305±1.3		
k_2 [d^{-1}]		**k_2 [d^{-1}]**			
80 and 85 °C		75–85 °C			
E_a [kJ mol^{-1}]	430.9	E_a [kJ mol^{-1}]	365.8±38		
Log (Z [d^{-1}])	62.052	Log (Z [d^{-1}])	52.52±5.6		

At low temperature values, the ML of ADN shows time-temperature dependence with an apparent linear increase typical for the zero order reaction (Figure 11) over the considered time range. Accelerative behavior can be found at longer aging times as is the case at 75 °C, see Figure 10. Figure 11 highlights the ML of ADN prills up to 200 d. Comparing with Figure 10 one can recognize the ML evolution after this time period. Examples of the modeling of the mass loss of the ADN prills are presented in Figure 12 and Figure 13.

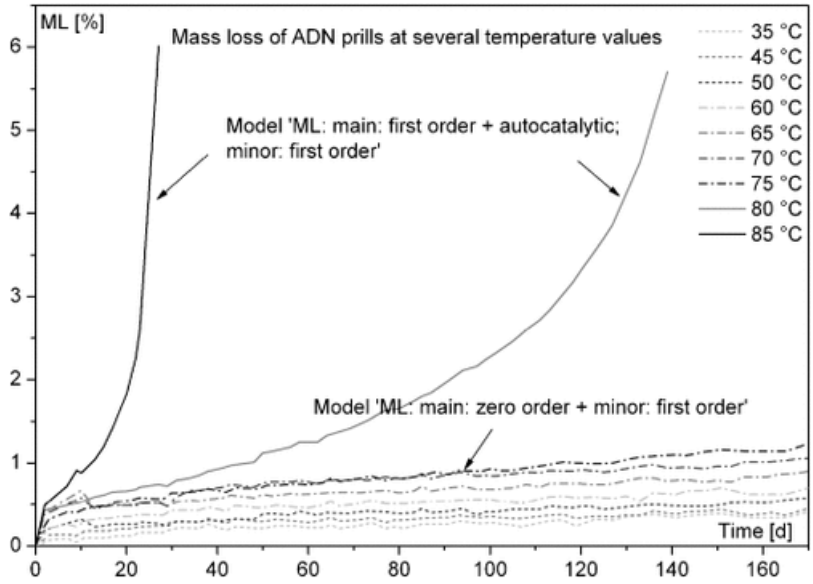

Figure 11 Mass loss of the ADN prills measured at high and low temperature values in the time range up to 200 days.

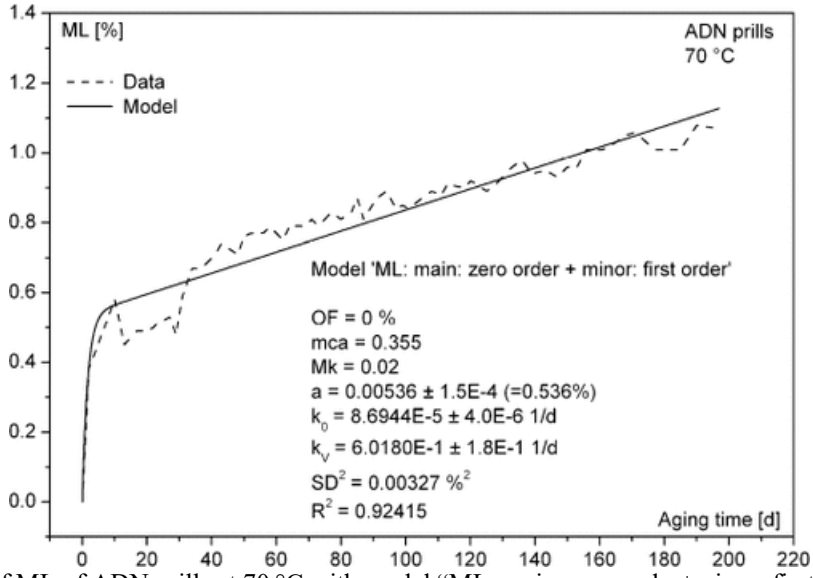

Figure 12 Modeling of ML of ADN prills at 70 °C with model “ML: main: zero order+minor: first order”.

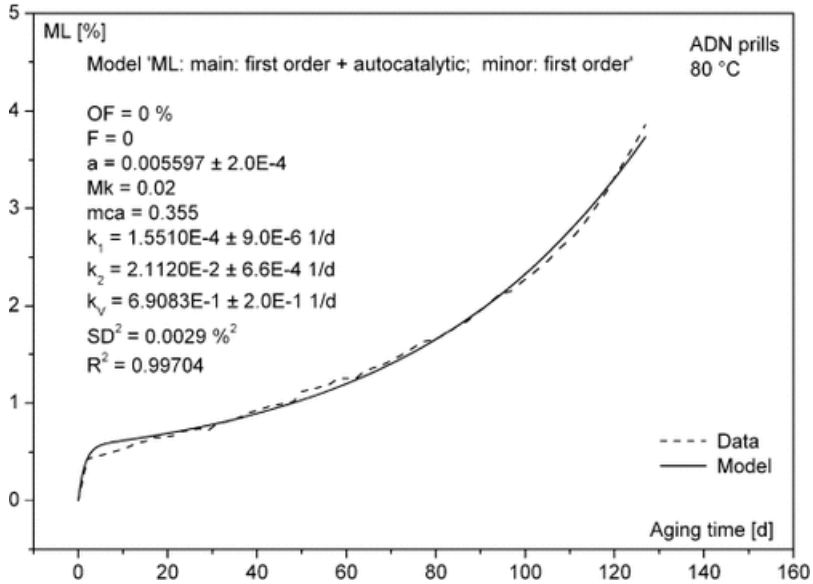

Figure 13 Modeling of the mass loss of ADN prills at 80 °C using the autocatalytical model.

Figure 14 and Figure 15 show the typical temperature behavior with aging of the investigated ADN-formulations. The considerations made before are valid also here. ADN-GAPxx propellants (Figure 14) show lower ML values and decompose in half the time if compared with the ADN-D2200xx propellant formulations (Figure 15).

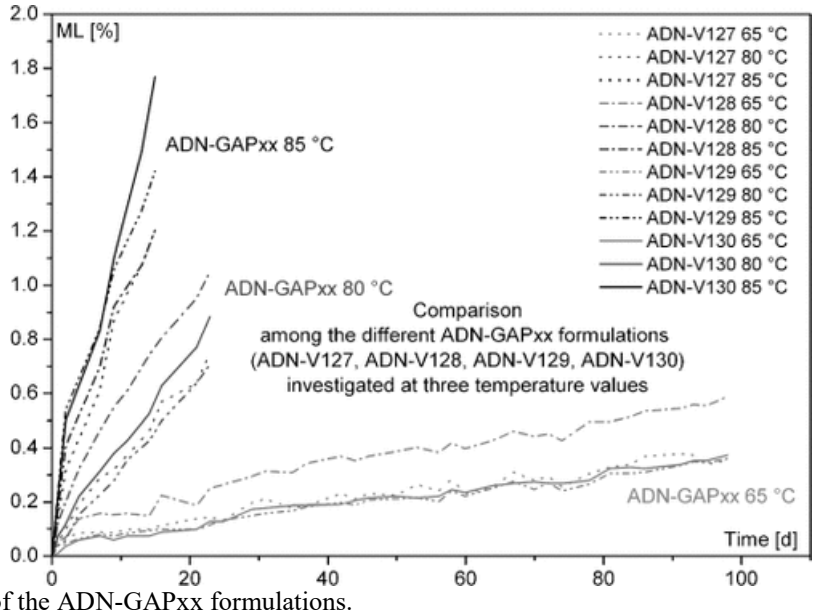

Figure 14 Mass loss of the ADN-GAPxx formulations.

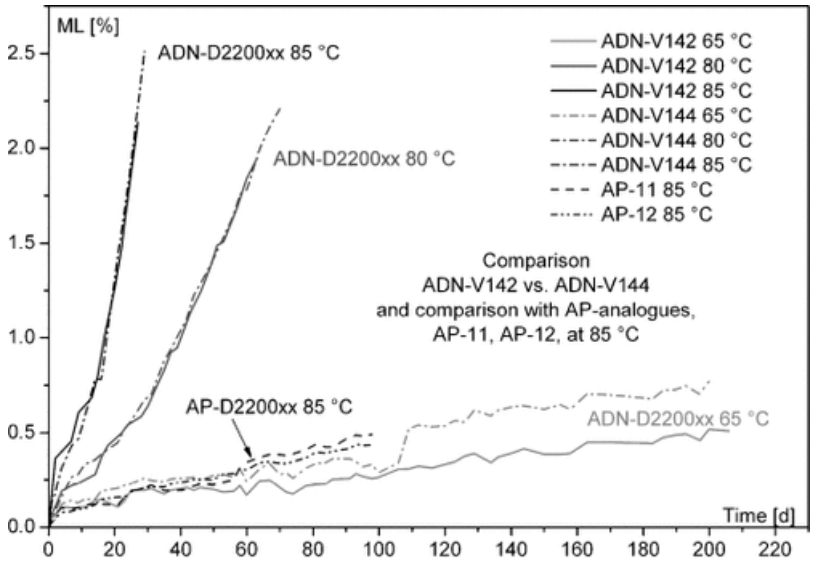

Figure 15 Mass loss of the D2200xx formulations.

4 Conclusion

Several ADN/GAP- and ADN/Desmophen®-based propellant formulations have been investigated, including comparisons with AP analogues.

GAP-based propellants do not have satisfactory mechanical properties. If compared with formulations containing Desmophen® D2200 as binder (ADN/Al, AP/Al, AP/HMX), these last ones have lower strain capabilities but higher maximum corrected stress values, whereas formulations containing ADN/HMX show no significant differences in maximum corrected stress values but higher strain capabilities. The effectiveness of the bonding agent (HX-880) was also studied, but negligible effects on the mechanical properties have been found. Moreover, some incompatibility problems with the ADN prills have also been observed. The replacement of BPS by Desmodur® N100 as curing agent for the GAP-diol pre-polymer showed a significant improvement of the

mechanical properties. The use of BPS turned out to be problematic, because it is impossible to control the inter-cross-linking chain lengths during the curing process. Consequently, unpredictable changes in the sliding lengths of the polymer chains occur.
SEM analyses of the ADN/GAP-based formulations showed evidence of a high porosity of the propellants and strong dewetting phenomena.
DMA measurements revealed high T_g values for all the investigated formulations. These values are 40 °C to 50 °C higher than the ones of the current HTPB/AP/Al-based formulations. Therefore they cannot fulfill the NATO specifications for the very wide in-service temperature range of −54 °C to +71 °C. The study has also underlined that filler and pre-polymer types, solid load content, replacement of ADN by AP and type of curing agent have influences on T_g and on the maximum of tanδ.
Finally, information about the aging behavior was obtained, too. ADN-based propellants showed remarkable chemical decomposition. Mass loss measurements revealed an acceleratory behavior at high temperature values, which is in part caused also by autocatalysis.

Symbols and Abbreviations

$\Delta\varepsilon_{log}$ Variation of the logarithmic strain, [%]
$\Delta\sigma_{corr}$ Variation of the corrected stress, [%]
ε_{log} Logarithmic or natural strain, [mm·mm^{-1}]
σ_{corr} Corrected stress, [N·mm^{-2}]
μAl Micrometric aluminum, 8 μm
ρ_{th} Theoretical density evaluated with the ICT-thermodynamic code, [g cm^{-3}]
ADN Ammonium dinitramide, oxidizer
Akardit II Stabilizer for nitrate esters; *N*-methyl, *N*′,*N*′-diphenyl urea; also called acardite II
Al Aluminum, fuel
AP Ammonium perchlorate, oxidizer
AN Ammonium nitrate
b.a. Bonding agent
BDNPA-F Bis(2,2-dinitropropyl)acetal/bis(2,2-dinitropropyl)formal, plasticizer
BPS Bispropargylsuccinate, curing agent
DMA Dynamic mechanical analysis
E_a Activation energy, [kJ mol^{-1}]
GAP Glycidylazide polymer, pre-polymer
HDI Hexamethylene diisocyanate, curing agent
HTPB Hydroxyl-terminated polybutadiene, pre-polymer
HX-880 *N*,*N*-Bis(2-Hydroxyethyl)glycolamide, referred as BHEGA, bonding agent
m.-% Mass-%
ML Mass loss
MNA Stabilizer for nitrate esters, N-methyl-*p*-nitroaniline
nAl Nano-aluminum, 100–200 nm
2-NDPA 2-Nitro-diphenylamine, stabilizer
NATO North Atlantic Treaty Organization
NCO Isocyanate group
O.B. Oxygen balance
OH Hydroxyl functional group
R_{eq} Equivalent ratio between the functional groups of curing agent and binder, [-]
SEM Scanning electron microscopy
STANAG Standardization agreement
tanδ Loss factor, [-]
T_g Glass transition temperature, [°C]

TMETN Trimethylolethyltrinitrate, plasticizer.

Acknowledgements

This work was carried out as part of the PhD Thesis of Sara Cerri done at Politecnico di Milano, Energy Dept. (Italy) and Fraunhofer ICT (Germany) 11. Authors would like to thank both institutions.

References

1. Cumming, Recent and Current NATO RTO Work on Munitions Disposal, *11th Int. Seminar New Trends and Research in Energetic Materials*, Pardubice, Czech Republic, April 9–11, 2008, p. 6–10.
2. S. Cerri, M. A. Bohn, K. Menke, L. Galfetti, Aging of HTPB/Al/AP Rocket Propellant Formulations Investigated by DMA Measurements, *Propellants Explos. Pyrotech.* 2013, 38, 190– 198.
3. T. Keicher, W. Kuglstatter, S. Eisele, T. Wetzel, H. Krause, Isocyanate-Free Curing of Glycidyl-Azyde-Polymer (GAP) with Bis-Propargyl Succinate (II), *Propellants Explos. Pyrotech.* 2009, 34, 210– 217.
4. K. Menke, T. Heintz, W. Schweikert, T. Keicher, H. Krause, Formulation and Properties of ADN/GAP Propellants, *Propellants, Explos. Pyrotech.* 2009, 34, 218– 230.
5. H. Pontius, J. Aniol, M. A. Bohn, Stability and Compatibility of a New Curing Agent for Binders Applicable with ADN Evaluated by Heat Generation Measurements, *6th Int. Heat Flow Calorimetry Symposium on Energetic Materials*, Pfinztal, Germany, May 6–8, 2008, p. 247–280.
6. U. Teipel, T. Heintz, H. Krause, Crystallization of Spherical Ammonium Dinitramide (ADN) Particles, *Propellants Explos. Pyrotech.* 2000, *25*, 81–85.
7. C. Boyars, K. Klager, Propellants Manufacture, Hazards, and Testing, Advances in Chemistry, Series 88, American Chemical Society, Washington DC, USA, 1969.
8. T. Heintz, A. Fuchs, Continuous Production of Spherical Ammonium Dinitramide Particles (ADN-Prills) by Microreaction Technology, *41st Int. Annual Conference of ICT*, Karlsruhe, Germany, June 29–July 2, 2010, p. 100.
9. S. Cerri, M. A. Bohn, K. Menke, L. Galfetti, Ageing Behaviour of HTPB Based Rocket Propellant Formulation, *Centr. Eur. J. Energ. Mater.* 2009, 6, 149– 165.
10. S. Cerri, M. A. Bohn, Ageing of HTPB/AP/Al Rocket Propellant Formulations Investigated by Dynamic Mechanical Analysis and Sol-Gel Analysis, *13th Int. Seminar New Trends and Research in Energetic Materials*, Pardubice, Czech Republic, April 21–23, 2010.
11. S. Cerri, *Characterisation of the Ageing of Advanced Solid Rocket Propellants and First Step Design of Green Propellants*, PhD Thesis, Politecnico di Milano, Dip. di Energia, Dottorato di Ricerca in Energetica, XXII Ciclo, 2011.
12. T. Heintz, M. Hermann, J. Aniol, A. Fuchs, Processing of Energetic Composite Particles by Fluidized Bed Technology, *41st Int. Annual Conference of ICT*, Karlsruhe, Germany, June 29–July 2, 2010, p. 99.
13. T. Heintz, K. Leisinger, H. Pontius, Coating of Spherical ADN Particles, *37th Int. Annual Conference of ICT*, Karlsruhe, Germany, June 27–30, 2006, p. 150.
14. T. Heintz, H. Pontius, J. Aniol, C. Birke, K. Leisinger, W. Reinhard, Ammonium Dinitramide (ADN)-Prilling, Coating and Characterization, *Propellants Explos. Pyrotech.* 2009, 34, 231–238.

15. M. A. Bohn, Generic Formulation of Performance Assessment Quantities for Stability Compatibility and Ageing of Energetic Materials, *14th Int. Seminar New Trends and Research in Energetic Materials*, Pardubice, Czech Republic, April 13–15, 2011, p. 46–77.
16. S. Cerri, M. A. Bohn, Ageing Behavior of Rocket Propellant Formulations with ADN as Oxidizer, *14th Int. Seminar New Trends and Research in Energetic Materials*, Pardubice, Czech Republic, April 13–15, 2011, p. 89–105.
17. T. Heintz, K. Leisinger, M. A. Bohn, Advanced Stabilization of ADN-Prills by Preparation of Raw Materials by Means of Fluidized Bed Technology, *43rd Int. Annual Conference of ICT*, Karlsruhe, Germany, June 26–29, 2012, p. 36.
18. S. Cerri, M. A. Bohn, K. Menke, L. Galfetti, Ageing of HTPB/Al/AP Rocket Propellant Formulations Investigated by DMA Measurements, Sol-Gel and GPC Analysis, *41st Int. Annual Conference of ICT*, Karlsruhe, Germany, June 29–July 2, 2010, p. 42.
19. *Military Agency for Standardization, Extreme Climatic Conditions and Derived Conditions for Use in Defining Design/Test Criteria for NATO Forces Material*, STANAG 2895, Edition 1, February 15, 1990.
20. S. Cerri, M. A. Bohn, K. Menke, L. Galfetti, Aging of ADN Rocket Propellant Formulations with Desmophen®-Based Elastomer Binder, submitted to *Propellants Explos. Pyrotech.* 2013.
21. M. A. Bohn, Kinetic Description of Mass Loss Data for the Assessment of Stability, compatibility and Aging of Energetic Components and Formulations Exemplified with ε-CL20, *Propellants Explos. Pyrotech.* 2002, *27*, 125–135.
22. G. B. Manelis, Thermal Decomposition of Dinitramide Ammonium Salt, *26th Int. Annual Conference of ICT*, Karlsruhe, Germany, July 4–7, 1995, p. 15.
23. M. A. Bohn, Modelling of the Stability, Ageing and Thermal Decomposition of Energetic Components and Formulations Using Mass Loss and Heat Generation, *27th Int. Pyrotechnics Seminar*, Grand Junction, CO, USA, July 16–21, 2000, p. 751–770.
24. M. A. Bohn, Stabilization of the New Oxidizer Ammonium Dinitramide in Solid Phase, *8th Int. Seminar EuroPyro 2003* of the "Groupe de Travail de Pyrotechnie", combined with the *30th International Pyrotechnics Seminar*, Saint Malo, France, June 23–27, 2003, p. 274–291.
25. M. A. Bohn, M. E. Grillo, Quantum Mechanical Calculations Used to Reveal Decomposition Ways of Ammonium Dinitramide (ADN), *37th Int. Annual Conference of ICT*, Karlsruhe, Germany, June 27–30, 2006, p. 74.
26. M. A. Bohn, P. Gerber, Stabilization of Solid ADN Liquid ADN-Aluminium Mixtures Suitable Stabilizing Substances Investigated by Heat Generation Rate, Mass Loss and Product Analyses, *9th. Int. Seminar EuroPyro 2007* of the "Groupe de Travail de Pyrotechnie", combined with the *34th International Pyrotechnics Seminar*, Beaune, France, October 8–11, 2007, p. 153–165.
27. A. I. Kazakov, Y. I. Rubtsov, G. B. Manelis, Kinetics and Mechanism of Thermal Decomposition of Dinitramide, *Propellants Explos. Pyrotech.* 1999, 24, 37– 42.
28. M. Rahm, *Green Propellants*, PhD Thesis, KTH Chemical Science and Engineering, Royal Institute of Technology, 2010
29. M. Rahm, T. Brinck, On the Anomalous Decomposition and Reactivity of Ammonium and Potassium Dinitramide, *J. Phys. Chem. A* 2010, 114, 2845– 2854.